Origin of Mountains on Io by Thrust Faulting and Large-Scale Mass Movements

Paul M. Schenk* and Mark H. Bulmer

Voyager stereoimages of Euboea Montes, Io, indicate that this mountain formed when a large crustal block was uplifted 10.5 kilometers and tilted by approximately 6 degrees. Uplift triggered a massive slope failure on the northwest flank, forming one of the largest debris aprons in the solar system. This slope failure probably involved relatively unconsolidated layers totaling approximately 2 kilometers in thickness, overlying a rigid crust (or lithosphere) at least 11 kilometers thick. Mountain formation on Io may involve localized deep-rooted thrust faulting and block rotation, due to compression at depth induced during vertical recycling of Io's crust.

Jupiter's moon Io is being volcanically resurfaced by lavas and plume deposits at such a high rate, estimated at about 1 cm/year (*1*), that crustal recycling is probably occurring on a global scale. Although mountains cover only a few percent of the surface and have no obvious global pattern (*2*), understanding whether these mountains formed by volcanic, compressional, or extensional processes may indicate how Io's crust is being recycled. These mountains and the manner in which they collapse or are eroded are also potential indicators of crustal strength and composition. Vast featureless plains, which cover nearly half the surface and surround these mountains, present a different problem in that it is not known whether they formed by deposition of effusive lava flows, plume-derived ash, or other materials.

Voyager obtained quality stereoimagery of roughly 40% of Io suitable for topographic mapping (*3*), which, together with recent Galileo observations (*4*), has led to a reexamination of the morphology and origin of Io's mountains. We report on the geology and topography of the prominent mountain Euboea Montes (Figs. 1 and 2), geomorphic evidence for mass movement there, and implications for mountain formation and for crustal stratigraphy and stability. The stereoimages used here (Fig. 1) have resolutions of 1.6 and 0.8 km/pixel. A digital elevation map (DEM) of Euboea Montes (Fig. 3) was generated from this stereopair, using an automated stereogrammetry program (*5*). The horizontal resolution of the DEM is ~8 km, the vertical resolution is ~250 m, and the formal errors associated with height measurements are ~300 m.

Euboea Montes (47°S, 336°W) is a roughly oval-shaped massif 175 km by 240 km, surrounded by smooth, nearly featureless plains on all sides. Within these plains are two low scarps 100 to 300 m high (Figs. 1 and 2). These scarps face away from Euboea and are located 0 to 70 km from the edge of the massif. They appear to be eroded margins of layered deposits, similar to those commonly observed on Io's smooth plains (*6*).

Euboea Montes can be divided into three geomorphic units (Figs. 1 and 2). A NE-SW–trending arcuate ridge crest or escarpment forms the spine of the massif. The highest elevation, 10.5 ± 1 km above the plains, occurs very near the center of this ridge crest, decreasing toward either end. This ridge crest divides the high Euboea massif into two sections. The southeast flank of the mountain is relatively steep and has a hummocky and striated surface. The northwest flank forms a smooth planar surface sloping uniformly at ~6° to the northwest. Two intact blocks (one 10 km by 100 km, the other ~10 km across) have broken away from the southwestern end of Euboea Montes and moved 3 to 5 km downslope.

Along the base of the planar northwest flank lies a thick, ridged deposit with lobate margins (Figs. 1 and 2). The ridges are a few kilometers wide and up to 50 km long, and are oriented parallel to the downslope direction. In some cases, prominent ridges appear to form the margins or levees of individual lobes within this deposit. Along its upslope or proximal margin, the ridged deposit stands ~6 km above the plains, sloping gently and uniformly toward the distal toe. The toe of the deposit is roughly 3.5 km thick near the midpoint, decreasing to 2 km toward the northeast and southwest ends of the deposit, and the whole deposit is 70 km by 200 km, covering an area of ~14,800 km^2.

Schaber (*2*) and Moore (*7*) suggested that the thick, ridged deposit could be due to either viscous volcanic flow or slumping [perhaps from creep induced by high heat flow (*7*)]. Using the stereoimages and topographic data, we found that the morphology at Euboea is most consistent with slope failure along the entire face of the northwest flank, forming a massive debris apron at the base of the mountain. We observed no evidence for lava flows, vents, calderas, or any other volcanic features within the ridged unit. The lobes and longitudinal ridges on the apron resemble those observed at slope failures on Earth, Mars, and the moon (*8*–*11*). Also, the width and thickness of the ridged deposit is directly corre-

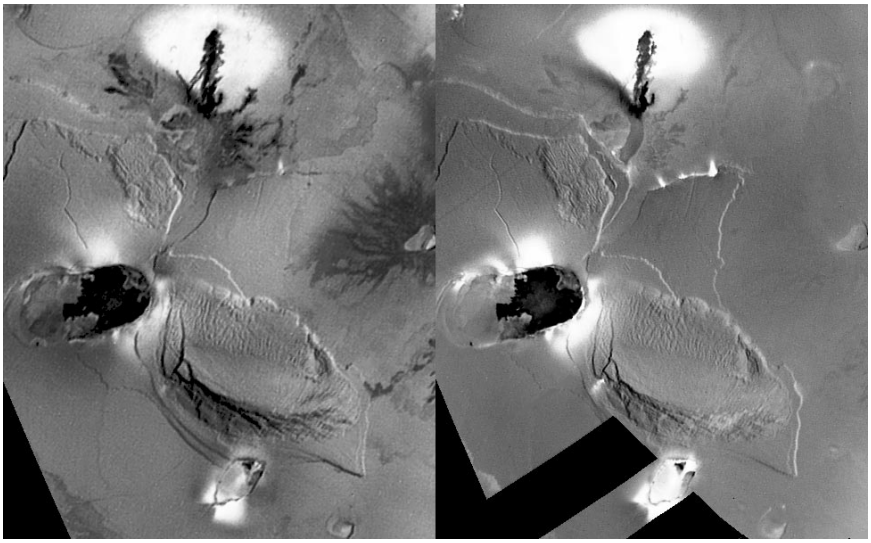

Fig. 1. Stereoimage pair of Euboea Montes, Io, obtained from Voyager 1 in 1979. Euboea Montes is the large massif near image center; Creidne Patera is the oval caldera with dark lava flows at center left adjacent to Euboea Montes. Voyager images FDS 16390.38 (right) and 16392.59 (left) are shown. Stereopair has a convergence angle of 49° and a base-to-height ratio of 1.5. Scene width is ~550 km. See Fig. 2 for north orientation and scale.

P. M. Schenk, Lunar and Planetary Institute, Houston, TX 77058, USA.
M. H. Bulmer, Center for Earth and Planetary Science, National Air and Space Museum, Washington, DC 20560, USA.

*To whom correspondence should be addressed. E-mail: schenk@lpi3.jsc.nasa.gov

lated with the height and width of the exposed northwest flank of Euboea Montes. This correlation is not expected for volcanic deposits and indicates that a layer of roughly uniform thickness failed and moved off the flank of Euboea Montes to form this deposit, producing a greater accumulation of debris where the original surface was wider (that is, the center of Euboea Montes).

Two types of slope failure are inferred from observations at Euboea Montes. The first is the massive debris apron along the northwest flank. Longitudinal ridges similar to those at Euboea occur in mass movement deposits in different environments and with a diverse range of compositions. On Earth, they occur on debris aprons in dry volcanic materials [Aucanquilcha volcano, Chile (*8*)], nonvolcanic materials [Carlson, Idaho (*12*)], ice [Altels, Austria (*13*)], and where there has been an ice or snow substrate [Sherman, Alaska (*9*)]. Extraterrestrial examples include Mars 1 in Ganges Chasma, Mars (*14*), and the deposit at Tsiolkovsky on the moon (*11*). Two possible origins have been proposed for longitudinal ridges. They may indicate divergent motion within the debris or the development of shear between substreams of debris traveling at different speeds (*9*).

These debris aprons are interpreted to be the product of rock and debris avalanches derived from bedrock escarpments. The motion of the debris need not require an interstitial mixture for support, but can rely in large part (when dry) upon grain-to-grain interaction generating a matrix material through fracturing and grinding associated with the avalanche event (*15*). We use the term "rock and debris avalanche" to describe an inertial granular mass derived from parent rock that does not require an interstitial sediment-water mix, trapped air, or hot volcanic gases.

The formation of the debris apron at the base of a planar surface 200 km across suggests that the northwest flank is an avalanche scar and that mass movement at Euboea Montes occurred along a distinct planar discontinuity within Io's crust after uplift and tilting (by ~6°) of the mountain. The orientation of rock layering and discontinuities plays a major role in mass movement (*16*). The slides at Vaiont, Italy (*17*), and Sherman, Alaska (*9*), occurred along bedding surfaces. Movement of material at Euboea may have occurred along a rheologic discontinuity between a weaker upper layer (which detached and formed the debris apron) and a more competent lower crustal layer (which forms the relatively intact Euboea massif): for example, a bedding contact between weak volcanic ash deposits and a mechanically stronger lower crustal layer [thermal metamorphism from Io's high heat flow (*1*) may strengthen unconsolidated materials at depth]. Alternatively, both upper and lower layers may have been competent and movement may have occurred along one or more distinct mechanical or stratigraphic planar discontinuities.

The volume of the debris apron on the northwest flank was estimated from the topography of the surface of the deposit. The precollapse surface was approximated by extrapolation of the planar surface of the northwest flank and the horizontal ground

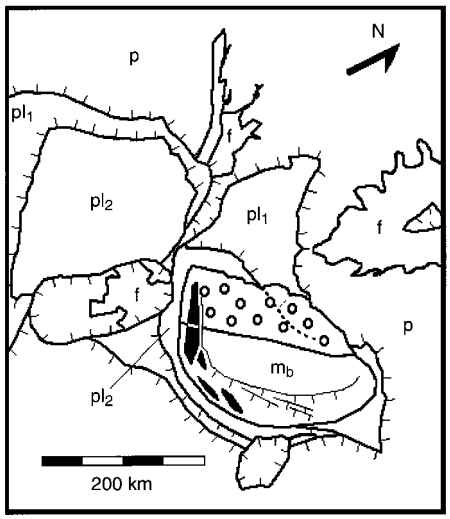

Fig. 2. Geologic sketch map of Euboea Montes based on Fig. 1. Geologic units are: lava flows (f), plains (p), layered plains (pl_1 and pl_2), basement massif material (m_b), ridged debris apron material (circles), and slumped blocks (dark units). Lines radiating from scarps indicate downslope direction. Dotted line indicates location of possible buried scarp described in text. Image location and map scale correspond to Figs. 1 and 3. N indicates north.

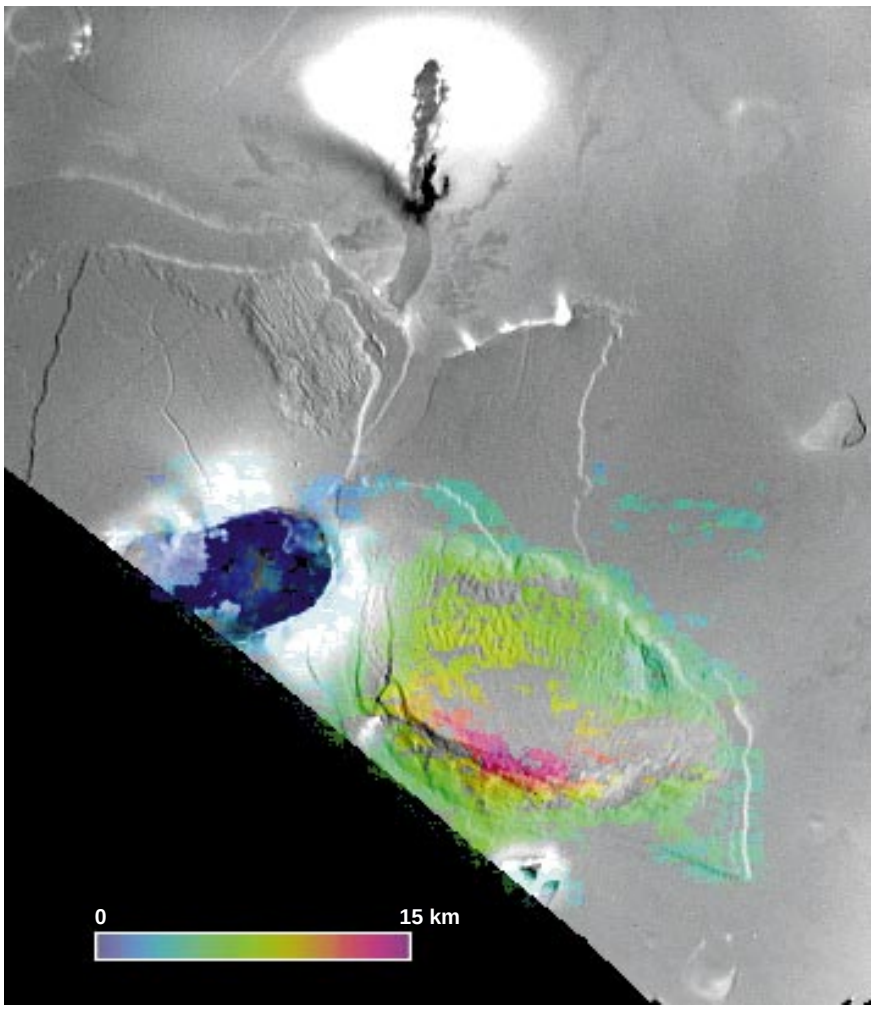

Fig. 3. Color-coded topographic map of Euboea Montes, derived from digital stereogrammetry (*5*). Color scale bar indicates relative elevations. Gaps in the data (uncolored areas) are where the stereogrammetric software failed to obtain a solution because of lack of detail or anomalous brightness patterns (*5*), or where data were not sampled. Image location and map scale correspond to Figs. 1 and 2.

plane. The estimated volume is ~25,000 km^3, which would make it the largest debris apron known in the solar system, with the possible exception of the Olympus Mons aureole deposits on Mars (*18*). If this volume is restored as a uniform layer over the entire surface of the tilted northwest flank (its proposed prefailure configuration), it would form a layer ~2 km thick. We propose that the two scarp-bounded 100- to 300-m-thick layers surrounding Euboea were part of the original stratigraphic sequence before uplift and were included in the material that formed the debris apron after uplift. If so, the estimated 2-km thickness of the debris apron material before failure may indicate the total thickness of these layered deposits in this region.

A minor break in slope within the Euboea debris apron may be related to an older plains scarp over which the material traveled. This scarp is a few hundred meters high and is one of the two that partially surround Euboea. The scarp stops where it intersects the toe of the debris apron, but a trace of it appears to continue under it toward the east, where it may reappear (Fig. 2). The parallel ridges within the debris apron disappear at the location of this buried scarp, suggesting that the behavior of the moving material changed when the apron traveled across the topographic scarp.

A large part of the toe of the debris apron was observed at 250 m resolution (Voyager FDS 16392.40). This surface has a homogeneous texture and appears to be free of blocks larger than ~500 m. This suggests that the material that formed the debris apron was poorly consolidated. This would tend to favor, although not require, the interpretation that the upper 2 km of crust forming the smooth plains are formed by relatively unconsolidated material such as volcanic ash [from Io's active plumes (*1*)] or ash interbedded with lava flows.

The maximum travel distance of the debris apron (from scarp crest to apron toe) is 130 km. Although this is a great distance compared with mass movements identified on Mars, Venus, or the moon (*10*), submarine debris aprons on Earth have traveled distances in excess of 150 km and often traveled over shallow slopes of <5° (*19*). The debris apron at Euboea follows the general correlation between greater descent height and greater run-out distance observed in avalanches on terrestrial planets (*20*). Using Coulomb's law of sliding friction and the displacement of center of mass, the coefficient of friction of a mass movement can be estimated by dividing the height (*H*) and the length (*L*) over which it traveled (*21*). The ratio *H*:*L* equals the tangent of the slope angle of the line connecting the top of the scarp to the toe of the apron (*13*). The *H*:*L* value for Euboea, which can be regarded as a mobility index for the debris apron, is 10.5:130 or ~0.08, which overlaps with values for debris aprons on Venus, Mars, the moon, and Earth (*20*). Taking into account the variations in environmental conditions on the different planets such as gravity, atmospheric density, pressure, and temperature, the distance that the Euboea apron traveled can be explained by the conversion of potential energy to kinetic energy. Essentially, the debris apron traveled as far as it did because of its large volume.

The second type of mass movement at Euboea Montes is represented by the intact blocks that detached from the southwestern end of Euboea (Fig. 1). These large blocks postdate the massive debris apron. They are similar to translational and possibly rotational failures and have analogs on the other terrestrial planets (*22*). Several smaller intact blocks a few kilometers across also appear to have toppled from the escarpment along the rugged southern flank of Euboea (Fig. 2).

We have stereoscopically measured the heights of several other mountains on Io. Boosaule Montes (height: 16 ± 2 km) has arcuate scarps that could be avalanche scars (*23*). Haemus Montes (height: 9 km) and a mountain 500 km west of Ra Patera [height: 4 to 5 km (*3*)] are characterized by numerous parallel and inclined striations. All lack any evidence of volcanic features. Whether the striations on these mountains are exposures of buried volcanic layers or parallel fracture planes is unknown, but tectonic activity is inferred to have raised these mountains to heights of >5 km. The relatively intact morphology of Euboea suggests that it may be an uplifted exposure of the crust of Io, which would then be at least ~13 km thick in this area (*24*). Uplift and rotation of crustal blocks may therefore be a common mechanism for mountain formation on Io. Although few mass movement features have been recognized on these mountains, the high volcanic resurfacing rate (*1*) could have buried such deposits.

The Ionian mountains described above have polygonal shapes, widths of 50 to 150 km, and inferred uplifts of 5 to 15 km, characteristics that are similar to those of basement-cored uplifts of the central Rocky Mountains in Wyoming (*25*) and the Sierras Pampeanas in Argentina (*26*). These mountains formed during uplift of coherent basement blocks up to 150 km long and are usually bound on one side by steeply dipping (30° to 70°) thrust faults penetrating through most of the crust. Faulting was apparently driven by regional compressional shortening of the crust (*25*, *27*). We suggest that uplift and rotation of Euboea Montes and possibly other mountains on Io may also have occurred as a result of horizontal compression and crustal shortening along deep-rooted thrust faults (*28*). At Euboea, this proposed thrust fault would be exposed along the southwest flank and dip steeply to the northwest beneath the massif. Striations along the southwest flank (Fig. 2) could be parasitic fractures splayed off the main thrust fault (*25*).

Based on these observations, inferences, and analogies, a scenario for the origin of mountains on Io is suggested. Galileo observations (*4*, *29*) suggest that over time, volcanism (or at least volcanic hot-spot distribution) occurs roughly uniformly over the surface. This implies that as new volcanic deposits are formed on the surface, older "layers" of similar age are forced to subside more or less uniformly into the interior. As this occurs, the effective radii of these global concentric layers decrease, placing the crust at depth under nonhydrostatic horizontal compressive stress. This global compression is relieved in quasi-random locations by deeply penetrating thrust faulting and uplift of large crustal blocks. Specific occurrences of failure may be triggered by anisotropies in the crust, as may be the case in the Rocky Mountains. (*25*), or by localized weakening or fracturing of the crust at volcanic centers, such as Creidne Patera, an 80 km by 170 km caldera located only 40 km southeast of Euboea (Fig. 1). This suggested scenario is potentially testable with high-resolution Galileo images of Io planned for 1999.

REFERENCES AND NOTES

1. A. McEwen *et al.*, in *Time-Variable Phenomena in the Jovian System* (NASA Spec. Publ. 494, NASA, Washington, DC, 1989), pp. 3–46; G. Veeder *et al.*, *J. Geophys. Res.* **99**, 17095 (1994).
2. G. Schaber, in *Satellites of Jupiter*, D. Morrison, Ed. (Univ. of Arizona Press, Tucson, AZ, 1982), pp. 556–597.
3. P. Schenk *et al.*, *Geophys. Res. Lett.* **24**, 2467 (1997).
4. M. Carr, *Geol. Soc. Am. Abstr. Programs* **29**, A-311 (1997).
5. This software was developed in 1995–96 at the Lunar and Planetary Institute by P. Schenk and B. Fessler for use with Voyager images and employs a scene-recognition algorithm to locate features in each image and determine parallax (*3*).
6. J. McCauley *et al.*, *Nature* **280**, 736 (1979); J. M. Moore *et al.*, *Icarus* **122**, 63 (1996).
7. H. J. Moore, *U.S. Geol. Surv. Misc. Investig. Map I-1851* (1987).
8. P. W. Francis and G. L. Wells, *Bull. Volcanol.* **50**, 258 (1988).
9. R. L. Shreve, *Science* **154**, 1639 (1966).
10. P. J. Shaller, thesis, California Institute of Technology, Pasadena (1991); M. H. Bulmer, thesis, University of London (1994).
11. J. E. Guest, in *Geology and Physics of the Moon*, G. Fielder, Ed. (Elsevier, Amsterdam, 1971), pp. 93–103.
12. P. J. Shaller, *Can. Geotech. J.* **28**, 584 (1991).
13. A. Heim, *Bergstruz und Menschenleben* (Fretz und Wasmuth, Zurich, 1932), p. 218.
14. B. Lucchitta, *Geol. Soc. Am. Bull.* **89**, 1601 (1978).

15. J. C. Yarnold, *ibid.* **105**, 345 (1993).
16. L. Muller, *Rock Mech. Eng. Geol.* **6**, 1 (1968).
17. B. Voight and W. Pariseau, in *Geotechnical Engineering*, B. Voight, Ed. (Elsevier, Amsterdam, 1978), pp. 1–67.
18. R. Lopes *et al.*, *J. Geophys. Res.* **87**, 9917 (1982); R. Lopes *et al.*, *Moon Planets* **22**, 221 (1980); P. W. Francis and G. Wadge, *J. Geophys. Res.* **88**, 8333 (1983); M. Bulmer and P. McGovern, *Lunar Planet. Sci.*, in press.
19. R. Dingle, *J. Geol. Soc. London* **134**, 293 (1977); C. Summerhayes *et al.*, *Mar. Geol.* **31**, 265 (1979).
20. See P. Schenk and M. Bulmer [*Lunar Planet Sci.* **XXVIII**, 1247 (1997)] and M. Bulmer (in preparation), and references therein.
21. The average friction coefficient is given by the tangent of the slope connecting the pre- and postevent centers of gravity of a failed mass (*30*). Because it is not possible to determine the pre- and postevent centers of gravity for masses on Io or most other planets, we use the tangent of the slope angle of the line connecting the top of the scarp to the toe of the apron (*13*) to derive the ratio *H*:*L*. The value derived using this method approximates the center of gravity gradient for those slope failures whose center of gravity lies near the toe (*10*), which may be the case for Euboea. Taking these caveats into consideration, we use *H*:*L* as an estimate of the coefficient of friction.
22. M. H. Bulmer and J. E. Guest, in *Volcano Instability on the Earth and Other Planets*, W. J. McGuire, A. P. Jones, J. Neuberg, Eds. (Geological Society of London, London, 1996), p. 349.
23. At 16 km height, Boosaule Montes (10°S, 270°W) is the highest mountain identified to date on Io. The automated stereogrammetry (*5*) measurement we report has been confirmed by manual measurement of parallax in the Voyager images.
24. Previous estimates that the crust of Io is ~30 km thick (*31*) assumed that mountain heights are due to isostatic buoyancy of material that is lower in density than the surrounding crust. Our interpretation of the formation of Euboea Montes suggests that mountains may have the same density as the surrounding crust, indicating that these crustal thickness estimates are not generally relevant to Io.
25. R. Allmendinger, in *Geology of North America—An Overview*, vol. G-3 of *Geology of North America*, B. Burchfiel, P. Lipman, M. Zoback, Eds. (Geological Society of America, Boulder, CO, 1992), pp. 583–608; D. Miller, T. Nilsen, W. Bilodeau, *ibid.*, pp. 205–260.
26. T. Jordan and R. Allmendinger, *Am. J. Sci.* **286**, 737 (1986).
27. S. Smithson *et al.*, *J. Geophys. Res.* **84**, 5955 (1979).
28. On Io, it is not known whether such faults penetrate the crust or the lithosphere.
29. R. Lopes-Gautier *et al.*, *Geophys. Res. Lett.* **24**, 2439 (1997); M. Carr, paper presented at the Lowell Observatory during the Galileo Era Conference, Flagstaff, AZ, 22 to 24 September 1997.
30. D. Cruden, *Geol. Soc. Am. Bull.* **91**, 63 (1980).
31. D. Nash *et al.*, in *Satellites*, J. Burns and M. Matthews, Eds. (Univ. of Arizona Press, Tucson, AZ, 1986), pp. 629–688.
32. This report is Lunar and Planetary Contribution No. 940. This work was done while M.H.B. was a Garber Fellow at the National Air and Space Museum. We are grateful to J. Moore, W. McKinnon, and an anonymous reviewer for comments.

31 October 1997; accepted 27 January 1998

Single-Grain ^{40}Ar-^{39}Ar Ages of Glauconies: Implications for the Geologic Time Scale and Global Sea Level Variations

Patrick E. Smith, Norman M. Evensen, Derek York, Gilles S. Odin

The mineral series glaucony supplies 40% of the absolute-age database for the geologic time scale of the last 250 million years. However, glauconies have long been suspected of giving young potassium-argon ages on bulk samples. Laser-probe argon-argon dating shows that glaucony populations comprise grains with a wide range of ages, suggesting a period of genesis several times longer (~5 million years) than previously thought. An estimate of the age of their enclosing sediments (and therefore of time scale boundaries) is given by the oldest nonrelict grains in the glaucony populations, whereas the formation times of the younger grains appear to be modulated by global sea level.

Glaucony (*1*) is an authigenic, millimeter-sized, greenish grain of marine clay consisting of aggregates of micrometer-sized crystallites. It is the only mineral facies that is sufficiently widespread to provide direct K-Ar and Rb-Sr ages for sediments. Glaucony is important for calibrating the geologic time scale because it provides ages in strata lacking reliable high-temperature chronometers (*2*), but glaucony ages have also been regarded as untrustworthy (*3*) because they are commonly too young. Glauconies are variable in composition because of a complicated authigenic evolution on the sea floor (*4*). Isotopic study indicated that immature, K-poor glauconies make poor chronometers, whereas evolved K-rich glauconies (>7 weight % K_2O) make the best dating material (*5*).

Glauconies used in the construction of modern time scales have undergone careful selection criteria (*6*). Although direct comparison of evolved glauconies to high-temperature minerals in a single well-understood stratigraphic section has not been possible, and although some high-temperature minerals may give anomalously old ages (*7*), slightly younger ages are apparent for time scales calibrated using glauconies (*7*) relative to scales constructed exclusively with high-temperature minerals (*8*). Consequently, some workers have chosen to ignore glauconies altogether in constructing their time scales. However, this strategy is unfortunate because glaucony is widespread in the geologic record and typically allows superior stratigraphic control.

The ability to date individual grains of glaucony by the ^{40}Ar-^{39}Ar method (*9*) allowed us to reexamine the use of glauconies for dating sediments. We investigated the uniformity of ages in three evolved bulk samples used to construct the geologic time scale (*10*), with K-Ar ages of about 20, 40, and 95 million years ago (Ma). For the single-grain dating, we used the technique of microencapsulation (*11*) to overcome the problem of loss of ^{39}Ar by recoil during irradiation (*9*). In parallel with the glauconies, we tested the reproducibility of 49 single grains of the sanidine age monitor Taylor Creek Rhyolite (TCR), which has crystal sizes small enough to yield individual age variances similar to those of the glauconies. The age distribution for TCR (Fig. 1) is singly peaked with a mean of 27.92 ± 0.05 Ma (*12*).

In contrast, the age distributions of the glauconies have multiple peaks (Fig. 1) with age ranges of ≥5 Ma (*13*). The color variations and wide ranges of ^{39}Ar recoil losses in the populations indicate that these samples contain grains that have been variably glauconitized, but there is no conspicuous relation between these parameters and a grain's age (Table 1). The question of which (if any) of the grains from a given population provide the best estimate of sedimentation age can only be answered by comparing their ages with presumably reliable and correlatable high-temperature mineral ages.

Each glaucony sample is taken from immediately above a stage boundary in the time scale. In each case, therefore, we can compare the ages of these samples to a set of high-temperature mineral ages drawn from rocks immediately below the same stratigraphic boundary (Fig. 1). The high-temperature minerals comprise all the ages in Harland *et al.*'s database (*14*) for the appropriate stages (Albian, Lutetian, and Aquitanian). The broad age distributions of these high-temperature minerals reflect not

P. E. Smith, N. M. Evensen, D. York, Department of Physics, University of Toronto, 60 St. George Street, Toronto, Ontario M5S 1A7, Canada.
G. S. Odin, Département de Géologie Sédimentaire, Université P. et M. Curie, 4 Place Jussieu, Case 119A, 75252 Paris Cedex 05, France.